

Temperature dependent gain of the atomic xenon laser

Gregory A. Hebner^{a)}

Sandia National Laboratories, Albuquerque, New Mexico 87185

Jong W. Shon and Mark J. Kushner

Department of Electrical and Computer Engineering, University of Illinois, 1406 W. Green Street, Urbana, Illinois 61801

(Received 2 August 1993; accepted for publication 23 September 1993)

Measured and calculated gain of the $1.73\ \mu\text{m}$ [$5d(3/2)_1-6p(5/2)_2$] and $2.03\ \mu\text{m}$ [$5d(3/2)_1-6p(3/2)_1$] atomic xenon transitions for gas temperatures between 290 and 590 K are presented. Fission-fragment excitation was used to generate the gain in Ar/Xe, He/Ar/Xe, and Ne/Ar/Xe gas mixtures at a pump power of $8\ \text{W}/\text{cm}^3$. For constant gas density, the gain exhibits an approximate T_{gas}^{-n} dependence with n between 2 and 3. The primary reactions responsible for the temperature dependence of the gain have been identified as dimer formation, dissociative recombination, and enhanced electron collisional mixing of the laser manifold due to an increased electron density.

The atomic xenon laser has demonstrated high efficiency with potential for quasicontinuous operation when excited by fission fragments.¹⁻³ Fission-fragment excitation, a subset of nuclear pumping techniques, utilizes the large kinetic energy of ^{235}U fission products to produce ionization and excitation in a gas mixture in much the same fashion as an electron beam. The relatively high energy loadings that can be obtained from fission-fragment excitation ($50-500\ \text{mJ}/\text{cm}^3$) can produce significant gas temperature excursion ($90-900\ \text{K}$ for 760 Torr argon). Increases in gas temperature of this magnitude can strongly influence the laser efficiency. Konak *et al.*⁴ and Magda⁵ recently demonstrated that the output power of the 1.73 , 2.03 , and $2.63\ \mu\text{m}$ transitions of the atomic xenon laser are strongly temperature dependent. Using the $^3\text{He}(n,p)^3\text{H}$ pumping reaction with a combined fission-fragment energy of $0.75\ \text{MeV}$, Konak *et al.* measured a strong decrease in 2.03 and $2.65\ \mu\text{m}$ laser output with increasing gas temperature.⁴ The gas mixture was $^3\text{He}/\text{Ar}/\text{Xe}$ ($49.5/49.5/1$) at a constant density ($1\ \text{atm}$ at $293\ \text{K}$) while the laser cavity had an output coupling of 6% at $2.03\ \mu\text{m}$ and 9% at $2.65\ \mu\text{m}$. The pump power was approximately $30\ \text{W}/\text{cm}^3$. The $2.03\ \mu\text{m}$ laser energy was constant for gas temperatures between 293 and $423\ \text{K}$ and decreased to zero at $623\ \text{K}$. In contrast, the $2.65\ \mu\text{m}$ laser energy terminated at $523\ \text{K}$. Magda showed that for ^{235}U fission-fragment pumping, the 1.73 and $2.03\ \mu\text{m}$ laser output energies decreased to zero at a gas temperature of approximately $573\ \text{K}$.⁵ The gas mixture was $\text{He}/\text{Ar}/\text{Xe}$ ($49.825/49.825/0.25$) at a total pressure of $840\ \text{Torr}$ and energy deposition of $110\ \text{mJ}/\text{cm}^{-3}$.

Measurements of laser efficiency are useful to characterize the total system performance. However, small signal gain measurements provide more fundamental information on laser kinetics. While extensive measurements and calculations have recently been performed to characterize the gain and efficiency of the atomic xenon laser at gas temperatures less than $325\ \text{K}$,^{1-3,6} the functional dependence of

the gain at gas temperatures above $325\ \text{K}$ has not been investigated, irrespective of the pumping mechanism (electron beam or fission fragments). Potential operating conditions for atomic xenon laser based systems include high energy loadings and high gas temperature ($T_{\text{gas}} > 325\ \text{K}$). Therefore the results discussed below are applicable to both fission-fragment and electron beam pumped systems. In this letter we report the first gain measurements of the 1.73 and $2.03\ \mu\text{m}$ atomic xenon transitions at elevated temperatures in Ar/Xe, He/Ar/Xe, and Ne/Ar/Xe gas mixtures. The measurements are compared with predictions from a computer model to identify the important laser kinetics.

The gain probe lasers and the general experimental details have been discussed previously in detail.¹⁻³ Briefly, gains at 1.73 and $2.03\ \mu\text{m}$ were simultaneously measured by combining two probe lasers using a dichroic mirror. The combined probe beams were injected into a waveguide system and passed through the fission-fragment-excited volume. After transmission through the cell and the associated beam train, the two probe wavelengths were separated using a second dichroic beam splitter and detected using bandpass filters and InAs detectors.

To facilitate the measurement of gain at elevated temperatures, a new fission-fragment pumped cell was constructed. As with the previous cell, the new cell was side pumped by fission fragments originating from a $0.5\text{-}\mu\text{m}$ -thick $^{235}\text{UO}_2$ coating on two plates ($10\times 60\ \text{cm}$). The excitation volume was $60\ \text{cm}$ long, $7\ \text{cm}$ high, with a plate spacing of $2.5\ \text{cm}$. The Sandia National Laboratories SPR-III reactor was used as a source of fast neutrons which were moderated to thermal values by a ceramic moderator. The cell and all other heated components were stainless steel with standard copper gasket seals. Windows (7940 quartz) were located at both ends of the cell and separated from the heated cell by a 7.5-cm -long, 3.2-cm -diam tube with an integral water jacket. The water jacket kept the Viton window seals below $325\ \text{K}$ even when the cell was heated to $575\ \text{K}$. Cell and gas temperatures were monitored by multiple thermocouples located inside and outside the cell. A turbomolecular pump was used to evacuate the

^{a)} Author to whom correspondence should be addressed.

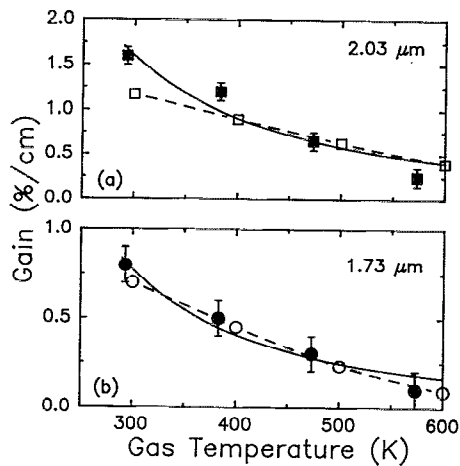


FIG. 1. Measured and calculated gain at (a) 2.03 and (b) 1.73 μm as a function of gas temperature. The gas mixture was Ar/Xe(99.7/0.3) at 260 Torr. Pump power was 8 W/cm³. Measured values are solid symbols and code predictions are open symbols. The solid line is the best fit to Eq. (1) and the dashed lines are a spline fit to the code predictions.

cell between reactor pulses and during substrate baking. Typically, the cell was filled with a new gas mixture 5 min before the reactor pulse. The UO₂-bearing substrates were baked under vacuum at 575 K for several days. During this time, measurements indicated that the gain steadily improved, presumably as water vapor and other impurities were driven from the substrates and the walls. After several days no further improvements in gain were observed and the gain data were reproducible during daily operation over a two week period.

Due to the difficulty of measuring the low energy deposition used in these experiments (less than 5 mJ/cm³), the pump power was inferred using two methods. First, measured room temperature gain was used to derive a peak pump power utilizing previous measurements of gain as a function of pump power.¹⁻³ Second, calculated coupling coefficients for neutron fluxes from the reactor to the laser cells were used to infer a pump power. These two techniques yield a peak pump power of 8 ± 2 W/cm³. The uncertainty in the measured gain is 0.1 cm⁻¹. To ensure a constant peak pump power for the variety of gas mixtures investigated, the pressures of the He/Ar/Xe and Ne/Ar/Xe gas mixtures were adjusted to yield the same fission-fragment stopping range as the Ar/Xe gas mixture.

Gain as a function of gas temperature for the experimental conditions was also investigated using the computer model described in Ref. 6. Briefly, the model is an accounting of heavy particle and electron kinetics in a particle beam excited plasma. A Monte Carlo simulation is used to generate excitation rates and electron temperatures. The plasma chemistry model addresses He/Ne/Ar/Xe gas mixtures while including 21 atomic levels in Xe to resolve gain at 1.73, 2.03, 2.63, 2.65, and 3.37 μm . Temperature dependent state-to-state quenching coefficients are included using detailed balance for endothermic processes in the absence of experimental data.⁷

Examples of the measured gain at 1.73 and 2.03 μm are shown in Figs. 1 and 2 for Ar/Xe and He/Ar/Xe gas

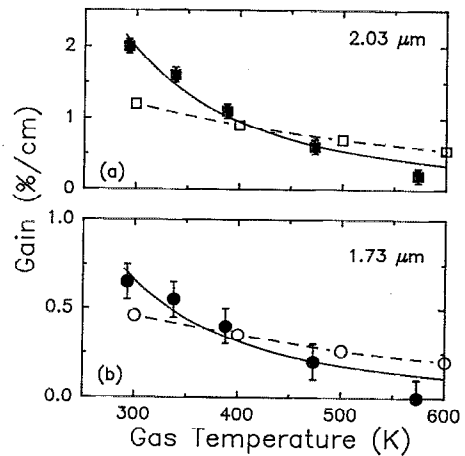


FIG. 2. Measured and calculated gain at (a) 2.03 and (b) 1.73 μm as a function of gas temperature. The gas mixture was He/Ar/Xe (49.8/49.9/0.3) at 430 Torr. Pump power was 8 W/cm³. Measured values are solid symbols and code predictions are open symbols. The solid lines are the best fit to Eq. (1) and the dashed lines are a spline fit to the code predictions.

mixtures, respectively. For all experiments, gas density was fixed at the room temperature value; as the cell temperature was increased, the pressure of the gas was increased to maintain a constant density. In the following discussion, the density is expressed in terms of the cell pressure at room temperature. The Ar/Xe (99.7/0.3) gas mixture had a total gas pressure of 260 Torr (293 K). The He/Ar/Xe (49.8/49.9/0.3) gas mixture had a total pressure of 430 Torr (293 K). The pump power was 8 W/cm³ for all cases. As the gas temperature increased from 290 to 570 K, gain at both 1.73 and 2.03 μm monotonically decreased. The magnitude of the decrease is consistent with the results of Magda and Konak who measured laser power as a function of temperature.^{4,5} In this regard, for all gas mixtures investigated, the gain at 570 K dropped below threshold for the laser cavity described by Konak.⁴

Predictions for gain from the model are also shown in Figs. 1 and 2. The calculated results have been normalized to the experimental values at $T_{\text{gas}}=400$ K to account for uncertainties in the pump rate since gain is quite sensitive to pump rate at low power deposition. For example, in one case, the computed gain varied between 2.2%/cm to 5.2%/cm over the range in uncertainty of pump power, 8 ± 2 W/cm³. The unnormalized calculated gain was within 50% of the experimental values at the nominal pump rate of 8 W/cm³.

The temperature dependence of calculated and measured gain are generally in good agreement. These trends can be explained by the temperature dependence of association and recombination reactions, and their effect on the electron density. The increase in gas temperature decreases the rate coefficients for three body association reactions (e.g., $\text{Ar} + \text{Xe}^+ + M \rightarrow \text{ArXe}^+ + M$). The temperature dependence of the three body association rate has been estimated from previous parametric studies to be $T_{\text{gas}}^{-1.5}$. Since dissociative recombination of ArXe⁺ is an important precursor to the upper laser level, lowering the three body

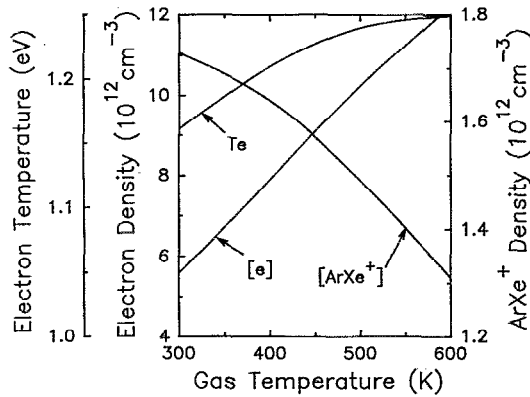


FIG. 3. Predications for electron density, ArXe⁺ density, and electron temperature for the conditions in Fig. 1.

association rate will decrease the pump rate. This effect is magnified by the fact that the rate of dissociative recombination (e.g., ArXe⁺ + e → Ar + Xe**) also decreases with increasing gas temperature, thereby further reducing the pumping of the upper level. Since the ionization rate is little affected by gas temperature, the decrease in dimer ion association and dissociative recombination of dimer ions also causes the electron density to increase with increasing gas temperature. This results in additional electron collision mixing (ECM) of the upper and lower laser manifolds, which reduces or quenches the inversion of the 1.73 and 2.03 μm transitions. These trends are shown in Fig. 3 where the computed electron density, ArXe⁺ density, and electron temperature are shown as a function of gas temperature. The ArXe⁺ density decreases while the electron density increases, resulting in a lower rate of pumping of the upper level, while ECM reduces or quenches the inversion. We also note an increase in T_e resulting from some additional recombination heating. The rates of endothermic heavy particle quenching reactions [e.g., Ar + Xe(6p[3/2]₁) → Ar + Xe(6p[3/2]₂)] also increase somewhat with increasing gas temperature but are not particularly important.

Experimental data were fit to a functional dependence of the form

$$g_0(T_{\text{gas}}) = g_0(293 \text{ K}) \left(\frac{(293 \text{ K})}{T_{\text{gas}}(\text{K})} \right)^n, \quad (1)$$

where $g_0(293 \text{ K})$ is the gain at room temperature and T_{gas} is the gas temperature. The gain at room temperature and n were obtained by a least-squares fitting routine. These values are shown in Table I for 1.73 and 2.03 μm. The table also includes the fits to additional He/Ar/Xe and Ne/Ar/Xe gas mixtures.

Gain was also measured at 470 K in a 260 Torr Ar/Xe gas mixture while varying the xenon concentration be-

TABLE I. Experimentally derived fit parameters to Eq. (1). The uncertainty in the fit is shown in parentheses.

Gas mixture	Ratio	Pressure		
		(Torr)	g_0 (%/cm at 293 K)	n
1.73 μm				
Ar/Xe	99.7/0.3	260	0.82(0.07)	2.3(0.4)
Ne/Ar/Xe	66.4/33.3/0.3	390	0.74(0.03)	2.5(0.2)
He/Ar/Xe	49.8/49.9/0.3	430	0.70(0.08)	2.6(0.7)
He/Ar/Xe	74.7/25.0/0.3	520	0.50(0.08)	3.0(0.8)
2.03 μm				
Ar/Xe	99.7/0.3	260	1.7(0.2)	2.0(0.5)
Ne/Ar/Xe	66.4/33.3/0.3	390	1.9(0.1)	2.6(0.1)
He/Ar/Xe	49.8/49.9/0.3	430	2.1(0.1)	2.5(0.4)
He/Ar/Xe	74.7/25.0/0.3	520	1.7(.04)	3.5(0.2)

tween 0.03% and 3%. As with previous data obtained at room temperature, the gain showed a broad maximum for xenon concentrations between 0.1% and 0.5%.^{1,3} These results imply that neutral collisional kinetics, which largely determined the laser performance as a function of gas mixture, are not severely affected by changes in gas temperature. This supports our contention that temperature dependent gain is largely a consequence of electron ion and ion molecule processes.

In conclusion, the gain of the 1.73 and 2.03 μm atomic xenon transitions has been measured and calculated for Ar/Xe, He/Ar/Xe, and Ne/Ar/Xe gas mixtures at gas temperatures between 290 and 570 K. Agreement between experiment and theory is generally good. Our results confirm that the gas temperature dependent performance of the high pressure atomic xenon laser is largely influenced by ECM and reduced excitation of the upper laser level due to a decreased rate of dimer formation and dissociative recombination.

We would like to acknowledge numerous discussions with G. N. Hays and W. J. Alford. The technical assistance of T. W. Hamilton, D. C. Meister, M. J. Johnson, and the SPR-III operations staff was critical to this work. The experiments were performed at Sandia National Laboratories and supported by the United States Department of Energy under Contract No. DE-AC04-76PD00789.

¹G. A. Hebner and G. N. Hays, J. Appl. Phys. **73**, 3614 (1993).

²G. A. Hebner and G. A. Hays, J. Appl. Phys. **73**, 3627 (1993).

³G. A. Hebner and G. N. Hays, J. Appl. Phys. **74**, 3673 (1993).

⁴A. I. Konak, S. P. Melnikov, V. V. Porkhaev, and A. A. Sinyanskii, Specialist Conference on the Physics of Nuclear Induced Plasmas and the Problems of Nuclear Pumped Lasers, Obninsk, Russia, May 1992 (unpublished).

⁵E. P. Magda, in Ref. 4.

⁶J. W. Shon, M. J. Kushner, G. A. Hebner, and G. N. Hays, J. Appl. Phys. **73**, 2686 (1993).

⁷A. P. Hickman, D. L. Huestis, and R. P. Saxon, J. Chem. Phys. **98**, 5419 (1993).